Injection molding for manufacturing of solid poly(L-lactide-co-glycolide) microneedles

Andrew Sachan¹, Roger J. Sachan², Junqi Lu², Huiying Sun², Yingai J. Jin², Detlev Erdmann³, Jennifer Y. Zhang², Roger J. Narayan^{4*}

*Corresponding author: Roger J. Narayan

UNC/NCSU Joint Department of Biomedical Engineering

Raleigh, NC 27695-7115 USA

T: 1 919 696 8488

E: roger narayan@unc.edu

¹ Wake Technical Community College, Raleigh, North Carolina, USA

² Department of Dermatology, Duke University Medical Center, Durham, North Carolina, USA

³ Division of Plastic, Maxillofacial and Oral Surgery, Duke University Medical Center, Durham, North Carolina, USA

⁴ Joint Department of Biomedical Engineering, the University of North Carolina and North Carolina State University, Raleigh, North Carolina, USA

Abstract:

A solid microneedle array can be used for "poke and flow" transdermal delivery of a drug, which involves the infusion or diffusion of a drug through pores in the skin that were created by the microneedle array. In this paper, solid microneedle arrays were created out of the polymer RESOMER LG 855 S - poly(L-lactide-co-glycolide) using injection molding. Scanning electron microscopy revealed that the microneedle in the injection-molded four-by-one microneedle array closely matched the dimensions that were used for injection molding. X-ray photoelectron spectroscopy revealed that the carbon bonding in the microneedle material matched that expected for poly(L-lactide-co-glycolide). The reduced elastic modulus of the microneedle material, 6.04 +/- 0.17 GPa, was noted to be appropriate for skin penetration applications. The microneedle array was used for the delivery of the model drug methyl blue to surgically-discarded human underarm skin. These results suggest that injection molding of RESOMER LG 855 S - poly(L-lactide-co-glycolide) may be an appropriate approach for large-scale manufacturing of solid microneedles.

Introduction:

Microneedles are needle-shaped microscale devices that may be used to create pores in the skin for the transdermal delivery of pharmacologic agents [1-6]. Drug delivery using microneedle devices was patented by Gerstel and Place in 1976 [7]. Microneedles exhibit several advantages over other technologies for transdermal drug delivery. The application of microneedles to the skin is associated with little or no pain since the microneedles do not have significant interaction with large nerve endings that a located in the dermis [2]. Bleeding and other tissue damage at the microneedle application site are minimal due to the small dimensions of the devices.

Solid microneedles create pores in the 15 µm-thick stratum corneum layer of the epidermis, enhancing the permeability of the stratum corneum layer and enabling the delivery of pharmacologic agents to deeper layers of the skin [4-6]. Several studies have demonstrated the functionality of solid microneedles for transdermal drug delivery. For example, Hao et al. described the use of eleven-by-eleven arrays of 800 µm microneedles for the delivery of small molecule drugs [8]. Zhang et al. used an array of solid polyglycolic acid microneedles to deliver an itraconazole-containing solution to a human basal cell carcinoma model that was regenerated on mice [9]. Itraconazole may inhibit the growth of basal cell carcinoma via inhibition of the Sonic Hedgehog (SHH) signaling pathway. Four-by-one arrays of 642 µm long polyglycolic acid microneedles with sharp tips were created using a process that involved injection molding and drawing lithography. Mice with a human basal cell carcinoma model were treated daily for two weeks with polyglycolic acid microneedle arrays and a solution containing itraconazole dissolved in 60% dimethyl sulfoxide and 40% polyethylene glycol-400 solution. The epidermal tissue treated with polyglycolic acid microneedles was much thinner than that of the untreated graft tissue. This study indicated that the solid polyglycolic acid microneedle array may be used to deliver itraconazole for localized treatment of basal cell carcinoma. More recently, acrylate-based polymer microneedle arrays that were created using a combination of two photon polymerization and micromolding were used to treat

cutaneous leishmaniasis in murine models [10]. A topical solution of amphotericin B dissolved in dimethyl sulfoxide was applied to microneedle-generated pores in BALB/c mice that were infected with *Leishmania mexicana* and *Leishmania major*. a statistically significant reduction of nodule sizes and parasite burden was noted for *Leishmania mexicana* lesions but not for *Leishmania major* lesions, which were associated with rapid progression of the infection.

In this study, injection molding was used to prepare microneedle arrays out of the biodegradable polymer poly(L-lactide-co-glycolide). This polymer, which is resorbed by the body, is used in medical devices such as orthopedic fixation devices and soft tissue fixation devices. The parameters for injection molding of this polymer, including thermomechanical parameters and injection-molding processing considerations, were described by Salmoria et al. and de Melo et al. [11, 12]. Scanning electron microscopy, energy-dispersive X-ray spectroscopy, X-ray photoelectron spectroscopy, nanoindentation, and a skin penetration study with discarded human skin were used to evaluate the microneedle arrays. The results of this study show the promise of injection-molded solid poly(L-lactide-co-glycolide) microneedle arrays, which can be made inexpensively and in large quantities, for the delivery of pharmacologic agents.

Experimental Procedure:

The four-by-one microneedle arrays were produced via injection molding using RESOMER LG 855 S poly(L-lactide-co-glycolide) (Evonik Rohm GmbH, Essen, Germany) at Evonik's Medical Device Center (Birmingham, AL). The design of the microneedle array is shown in Figure 1 (a); the microneedles were designed with a tip diameter of 0.4 mm and a base diagonal of 2.1 mm. RESOMER LG 855 S is a semi-crystalline ester-terminated polymer contains a lactide:glycolide ratio of 85:15 and exhibits a viscosity of 2.5-3.5 dL/g, melting point of 159-166 °C, and glass transition temperature (T_g) of 53-63 °C.

Imaging of the microneedles was performed using a Hitachi S3200N variable pressure scanning electron microscope (Hitachi, Tokyo, Japan). An Oxford energy dispersive X-ray spectrometer was used to collect

energy-dispersive X-ray spectroscopy from the microneedle tip. An Au/Pd coating was then deposited on the microneedle array using a sputtering system; images were subsequently obtained from the microneedle array. X-ray spectroscopy data was obtained using a XPS/UVS SPECS System with PHOIBOS 150 Analyzer (SPECS Surface Nano Analysis GmbH, Berlin, Germany). Reduced modulus and hardness values were obtained from a flat region on the opposite side from the base as the microneedle array using a Bruker Hysitron TI980 Triboindenter (Billerica, MA). A diamond conospherical (conical) tip with a 1 µm radius of curvature was used in this study. The sample was tested six times to a max load of 1mN. A load time of 5 s, a hold time at maximum load of 2 s, and an unload time of 5 s was used in this study.

Surgically discarded human underarm skin was obtained from plastic surgery from Duke Hospital in accordance with the Institutional Review Board protocol approved by Duke University. The subcutaneous fat tissues were removed by surgical tweezers and scissors. The surface of the skin was then cleaned with phosphate-buffered saline, wiped dry using Kimwipe, and laid flat on a petri dish. 200 μl 1% methyl blue in phosphate-buffered saline was pre-loaded on the skin, and the epidermal side was perforated by the microneedle array. The surface of the skin was wiped again to eliminate excess methyl blue. The upright brightfield image of the needle point was photographed by the Olympus IX73 imaging system (Center Valley, PA). A 50 mm by 50 mm tissue block around the needlepoint was cut out, embedded in optimal cutting temperature (O.C.T.) compound, immediately frozen on dry ice, and kept in -80 °C freezer for freezing until sectioning. A series of 7 μm thick skin sections were cut on a cryostat microtome. The sections were then stained by 5 μg/ml Hoechst and photographed by brightfield and fluorescence (excitation 361 nm, emission 457 nm) Olympus BX41 microscopic imaging system (Center Valley, PA).

Results and Discussion:

Scanning electron micrographs of the four-by-one Resomer® LG 855 S microneedle array are shown in Figure 1 (b) shows a 40X image of a single microneedle, Figure 1 (c) shows a 40X image of a single microneedle at 45° tilt, and Figure 1 (d) shows a 200X image of a single microneedle at 45° tilt. Some artifacts of the injection molding process (e.g., flash at the microneedle tip) were noted in the images; these defects may be removed through additional processing of the microneedle arrays. Ten measurements of the microneedle tip, lateral edge, and base diagonal were made using ImageJ software (NIH, Bethesda, MD). The tip exhibited a diameter of 408.4 μ m, which was similar to the expected tip diameter of 0.4 mm. The base diagonal exhibited a length of 2064.4 μ m, which closely matched the expected base diagonal length of 2.1 mm. The lateral edge exhibited a length of 1780.2 μ m, which closely matched the expected length of 1839.8 μ m. In general, the measurements obtained from the scanning electron micrographs of the microneedle array closely matches the design of the microneedle array.

Energy-dispersive X-ray spectroscopy data from the microneedle tip revealed the presence of C, O, and 0.2% weight percent or less Si, Ca, Al, Na, or Cl. The X-ray photoelectron spectroscopy survey scan identified the presence of C, O, and Si in the microneedle array (Figure 2 (a)). None of the identified impurities (e.g., Si, Al, Na, or Cl) have concerns related to toxicity for skin contact applications. The X-ray photoelectron spectroscopy C1s spectrum showed peaks at bond energies of 289, 287, and 285 eV. These peaks in poly(L-lactide-co-glycolide) have been described by Hsu et al. and Shibata et al. as arising from carbon in the ester bond, carbon in the C–O bond, and carbon in the alkyl group, respectively [13, 14]. No carbon bonding that has not previously been identified with poly(L-lactide-co-glycolide) was noted in the sample.

Nanoidentation revealed that the microneedle material exhibited a reduced Young's modulus value of 6.04 +/- 0.17 GPa and a hardness value 371.88 +/- 27.5 MPa. Park et al. previously described poly(L-lactide-co-glycolide) microneedles that exhibited a Young's modulus value of 3 GPa; the noted that

microneedles made from materials with a Young's modulus values greater than ~1 GPa generally show fracture forces that exceed the forces needed for skin insertion [15].

Cryostat sectioning and histological visualization of the microneedle-treated discarded human skin have been a common approach to evaluate the penetration of microneedle arrays [16, 17]. The depth of the microneedle penetration was measured by Z-stacking on the upright view of the needlepoint with a step of 20 µm until the bottom was reached. This analysis showed that microneedle punch allowed dye penetration to be detected in a total of 19 stacks, amounting to 380 µm in depth (Figure 3 (a)). To verify this result, we sectioned the methyl-blue-treated skin around the needlepoint, stained cell nuclei with the florescent Hoechst 33342, and imaged the tissue under brightfield and fluorescence. The brightfield image of the cryosection showed that microneedle treatment resulted in an over 210 µm indentation and a rupture through the epidermis and achieved delivery of methyl blue to approximately 151 µm below the surface of the epidermis which is delineated by Hoechst-staining (Figure 3 (b-c)). This result indicated that the solid poly(L-lactide-co-glycolide) microneedle array was effective for human skin penetration and delivery of a model drug.

Conclusions:

The scanning electron microscopy showed that a microneedle in the microneedle array closely matched the dimensions (e.g., tip diameter, base diagonal, and lateral edge) of the design that was used for injection molding. Energy-dispersive X-ray spectroscopy and X-ray photoelectron spectroscopy revealed the presence of no toxic impurities; X-ray photoelectron spectroscopy revealed that the carbon bonding in the microneedle material matched that expected for poly(L-lactide-co-glycolide). The reduced elastic modulus of the microneedle material, 6.04 +/- 0.17 GPa, obtained through nanoindentation was noted to be appropriate for skin penetration applications. The microneedle array was successfully used for the delivery of the model drug methyl blue to surgically-discarded human underarm skin. These results

suggest that injection molding of RESOMER LG 855 S - poly(L-lactide-co-glycolide) may be an
appropriate approach for large-scale manufacturing of solid microneedles for transdermal drug delivery.
Conflict of interest statement:
On behalf of all authors, the corresponding author states that there is no conflict of interest.
Data availability:
The datasets generated during and/or analyzed during the current study are available from the corresponding author on reasonable request.
References:
1. R. J. Narayan, J. Biomed. Nanotechnol. 10, 2244 (2014).

- 2. P. Khanna, J. A. Strom, J. I. Malone, S. Bhansali, J. Diabetes Sci. Technol. 2, 1122 (2008).
- 3. S. H. Bariya, M. C. Gohel, T. A. Mehta, O. P. Sharma, J. Pharm. Pharmacol. 64, 11 (2012).
- 4. Y. C. Kim, J. H. Park, M. R. Prausnitz, Adv. Drug Deliv. Rev. 64, 1547 (2012).
- 5. A. Arora, M. R. Prausnitz, S. Mitragotri, Int. J. Pharm. 364, 227 (2008).
- 6. M. R. Prausnitz, R. Langer, Nat. Biotechnol. 26, 1261 (2008).
- 7. M. S. Gerstel, V. A. Place, Inventors; Alza Corp, Assignee. United States Patent 3,964,482. Jun 22 1976.
- 8. Y. Y. Hao, Y. Yang, Q. Y. Li, X. P. Zhang, C. B. Shen, C. Zhang, Y. Cui, X. D. Guo, J. Drug Target. 28, 811 (2020)
- 9. J. Zhang, Y. Wang, J. Y. Jin, S. Degan, R. P. Hall, R. D. Boehm, P. Jaipan, R. J. Narayan, JOM. 68, 1128 (2016).
- 10. A. K. Nguyen, K. H. Yang, K. Bryant, J. Li, A. C. Joice, K. A. Werbovetz, R. J. Narayan, Biomed. Microdev. 21, 8 (2019).
- 11. L. P. de Melo, G. V. Salmoria, E. A. Fancello, C. R. de Mello Roesler, Int. J. Biomater. 1256537 (2017).
- 12. G. V. Salmoria, L. F. Vieira, I. M. Gindri, C. R. Roesler, E. A. Fancello, Int. J. Adv. Manuf. Technol. 98, 2231 (2018).
- 13. S. T. Hsu, H. Tan, Y. L. Yao, Polym. Degrad. Stab. 97, 88 (2012).
- 14. A. Shibata, S. Yada, M. Terakawa, Sci. Rep. 6, 1 (2016).
- 15. J. H. Park, M. G. Allen, M. R. Prausnitz, J Control Release. 104, 51 (2005).
- 16. M. M. Badran, J. Kuntsche, A. Fahr, Eur. J. Pharm. Sci. 36, 511 (2009).
- 17. P. M. Wang, M. Cornwell, J. Hill, M. R. Prausnitz, J. Invest. Dermatol. 126, 1080 (2006).

Figure Captions:

Figure 1. (a) Image of the design of the four-by-one Resomer® LG 855 S microneedle array. Scanning electron micrographs of the four-by-one Resomer® LG 855 S microneedle array: (b) 40X image of a single microneedle, (c) 40X image of a single microneedle at 45° tilt, and (d) 200X image of a single microneedle at 45° tilt.

Figure 2. X-ray photoelectron spectra from Resomer® LG 855 S microneedle array. (a) survey spectrum. (b) C1s spectrum.

Figure 3. Light microscopy demonstrating the delivery of methyl blue with microneedle array in human skin. (A) Fused Z-stacks with a step of 20 μ m in the brightfield. (B) Brightfield image of the cryosection crosses the needle punch. (C) Fluorescence image of the Hoechst-stained cryosection. The white line denotes the board line between the dermis and epidermis. The white arrows indicate the point of skin rupture.

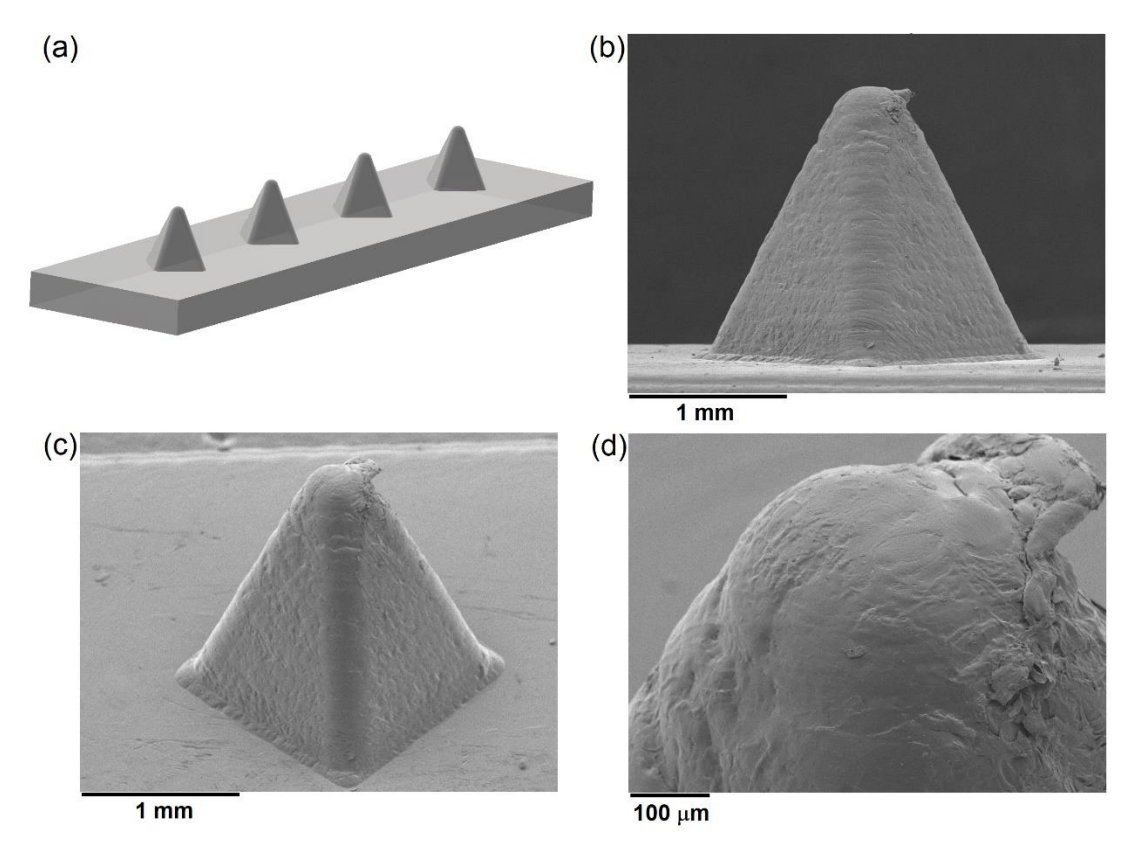


Figure 1.

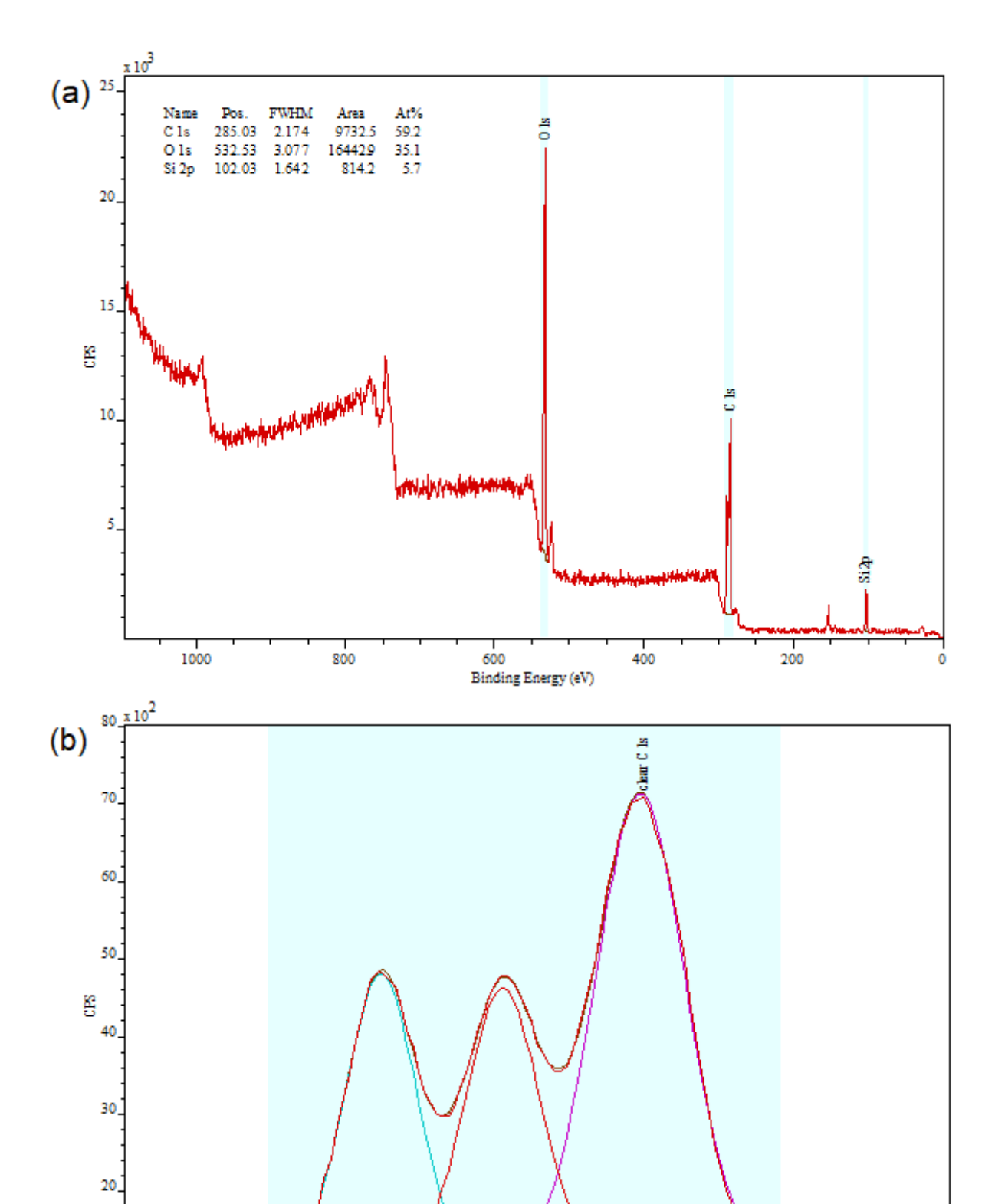


Figure 2.

Binding Energy (eV)

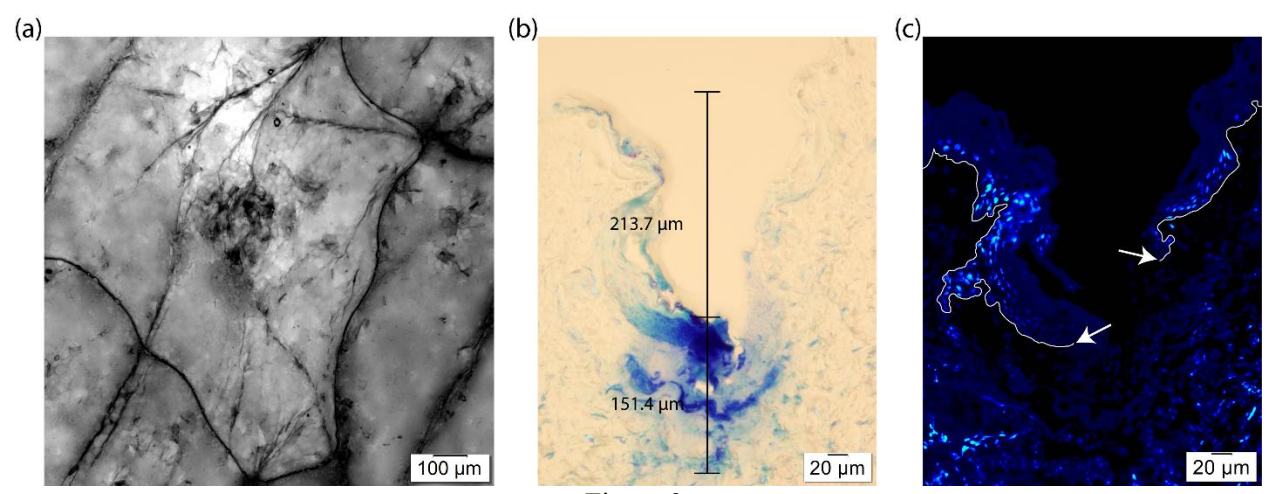


Figure 3.